(Nichirei, Tokyo, Japan) for immunostaining with antibodies against NFkB p65 (C20) (Santa Cruz Biotechnology, CA, USA) and MOMA2 (Serotec Immunological Excellence, Oxford, UK). Slides were next incubated with the biotinylated IgG for 1h and then with peroxidase-conjugated streptavidin for 30 min at room temperature. Finally, immunoreactivity was visualized by incubation with a substrate solution containing 3,3′-diaminobenzidine tetrahydrochloride (DAB). For experiments involving TNF-α induced p65 translocation, mice were injected with recombinant murine TNF-α (R&D Systems Inc, MN, USA), and killed 30 minutes later.

Immunoblotting

Lung samples obtained from mice were homogenized and subjected to immunoblotting as described previously.[5] Antibodies to IκB-α (C-15, 21) (Santa Cruz Biotechnology, CA, USA) were commercially obtained.

Quantitative RT-PCR–based gene expression

Total RNA was isolated from mouse tissues with Isogen (Wako Pure Chemical, Osaka, Japan), and cDNA was synthesized with a Cloned AMV First Strand Synthesis Kit (Invitrogen, MD, USA) using 5 μg of total RNA. cDNA synthesized from total RNA was evaluated using real-time quantitative PCR (Light Cycler Quick System 350S; Roche Diagnostics). The relative amount of mRNA was calculated with β-actin as the invariant control. Samples from skeletal muscle were calculated with α-actin as the invariant control. The oligonucleotide primers are described in Table S1. The mitochondrial DNA content was quantified using a sequence detection system (QIAGEN Inc., CA, USA). Total DNA was extracted from gastrocnemius muscles. The reactions were performed as follows: initial denaturing step at 95°C for 10 minutes and 40 cycles of 95°C for 15

seconds and 60°C for 1 minute. A melting curve was analyzed to check the specificity of the PCR product. The primer sequences were: 5'-GCC TTT CAG GAA TAC CAC GA-3'and 5'-CCA ATT TTA GGG GGT TCG AT-3' (GenBank NC 005089). The relative amounts of mitochondrial DNA were calculated with α-actin mRNA as the invariant control.

Oxygen consumption

Oxygen consumption was measured with an O2/CO2 metabolism measuring system (model MK-5000RQ; Muromachi Kikai, Tokyo, Japan) as described previously.[2]

Locomotor activity

Spontaneous locomotor activities of mice were analyzed with an infrared activity monitor (Supermex; Muromachi Kikai, Tokyo, Japan), as described previously.[6] In this system a sensor monitors motion in multiple zones of the cage and movement of animal in the X, Y and Z axis can be determined. Mice were first acclimatized to the cages and housed individually for 4 days before measurement were taken. Food and water were provided *ad libitum*. All counts were automatically recorded at 60-min intervals and totalled for both the 12- hour-light and 12-hour-dark period. Data were averaged over the 3-day period of measurement.

Muscle blood flow measurement

A catheter was inserted in the carotid artery for injection of fluorescent microspheres, a second one was inserted in the femoral artery for reference blood sample withdrawal. After stabilization of hemodynamic parameters, 200 μl of yellow-green fluorescent

microspheres (Triton, CA, USA) were injected into the carotid artery with an injection syringe over 10 s followed by 0.1 ml of saline. A reference blood sample was withdrawn from the femoral artery at a rate of 0.25 ml/min, into a pre-weighed heparinated syringe, starting 10 s before microsphere injection and lasting for a total of 60 s. The syringe containing the blood sample was weighed and the blood was digested with 250 μl of 16N KOH. Mice were sacrificed and skeletal muscles were weighed and digested in 4 ml of 4N KOH with 20% Tween 80. After 24 h, the digested tissues were filtered individually and processed for fluorescence quantification.[7]

Supplemental References

1. Hasegawa Y, Ogihara T, Yamada T, Ishigaki Y, Imai J, Uno K, Gao J, Kaneko K, Ishihara H, Sasano H, Nakauchi H, Oka Y, Katagiri H. Bone marrow (BM) transplantation promotes beta-cell regeneration after acute injury through BM cell mobilization. *Endocrinology.* 2007;148:2006-2015.
2. Ishigaki Y, Katagiri H, Yamada T, Ogihara T, Imai J, Uno K, Hasegawa Y, Gao J, Ishihara H, Shimosegawa T, Sakoda H, Asano T, Oka Y. Dissipating excess energy stored in the liver is a potential treatment strategy for diabetes associated with obesity. *Diabetes.* 2005;54:322-332.
3. Yamada T, Katagiri H, Ishigaki Y, Ogihara T, Imai J, Uno K, Hasegawa Y, Gao J, Ishihara H, Niijima A, Mano H, Aburatani H, Asano T, Oka Y. Signals from intra-abdominal fat modulate insulin and leptin sensitivity through different mechanisms: neuronal involvement in food-intake regulation. *Cell Metab.* 2006;3:223-229.
4. Uno K, Katagiri H, Yamada T, Ishigaki Y, Ogihara T, Imai J, Hasegawa Y, Gao J,

Kaneko K, Iwasaki H, Ishihara H, Sasano H, Inukai K, Mizuguchi H, Asano T, Shiota M, Nakazato M, Oka Y. Neuronal pathway from the liver modulates energy expenditure and systemic insulin sensitivity. *Science.* 2006;312:1656-1659.

5. Imai J, Katagiri H, Yamada T, Ishigaki Y, Suzuki T, Kudo H, Uno K, Hasegawa Y, Gao J, Kaneko K, Ishihara H, Niijima A, Nakazato M, Asano T, Minokoshi Y, Oka Y. Regulation of pancreatic beta cell mass by neuronal signals from the liver. *Science.* 2008;322:1250-1254.

6. Mashimo T, Voigt B, Kuramoto T, Serikawa T. Rat Phenome Project: the untapped potential of existing rat strains. *J Appl Physiol.* 2005;98:371-379.

7. Kubis N, Richer C, Domergue V, Giudicelli JF, Levy BI. Role of microvascular rarefaction in the increased arterial pressure in mice lacking for the endothelial nitric oxide synthase gene (eNOS3pt-/-). *J Hypertens.* 2002;20:1581-1587.

Supplemental Figure Legends

Supplemental Figure 1. Body compositions of $A^y/+$ control and E-DNIκB;$A^y/+$ mice

(A) Body weights of $A^y/+$ control (white bars) and E-DNIκB;$A^y/+$ (black bars) mice at 20 weeks of age. (B) Epididymal fat weights of $A^y/+$ control and E-DNIκB;$A^y/+$ mice at 20 weeks of age. (C) Liver weights of $A^y/+$ control and E-DNIκB;$A^y/+$ mice at 20 weeks of age. Data are presented as means ± SEM. *P<0.05 compared with $A^y/+$ control littermate group by one-way ANOVA. n=5 in $A^y/+$ control and n=6 in E-DNIκB;$A^y/+$ mice.

Supplemental Figure 2. Hepatic expressions of gluconeogenic genes from $A^y/+$ control and E-DNIκB;$A^y/+$ mice

Hepatic expressions of gluconeogenic genes from $A^y/+$ control (white bars, n=4) and E-DNIκB;$A^y/+$ (black bars, n=6) mice at 20 weeks of age were analyzed by RT-PCR. The relative amounts of mRNA were calculated with β-actin mRNA as the invariant control. Data are presented as means ± SEM.

Supplemental Figure 3. Adipose expressions of adhesion molecules and angiogenesis markers from $A^y/+$ control and E-DNIκB;$A^y/+$ mice

Expressions of adhesion molecules and angiogenesis markers in epididymal fat tissues from $A^y/+$ control (white bars, n=5) and E-DNIκB;$A^y/+$ (black bars, n=4) mice at 20 weeks of age were analyzed by RT-PCR. The relative amounts of mRNA were calculated with β-actin mRNA as the invariant control. Data are presented as means ± SEM. *P<0.05 compared with control littermate group by one-way ANOVA.

Supplemental Figure 4. Blockade of endothelial NF-κB signaling prevented insulin resistance in genetically obese (A^y/+) mice

Plasma levels of adipokines, inflammatory-related cytokines and insulin in A^y/+ control (white bars, n=5) and E-DNIκB;A^y/+ (black bars, n=6) mice were measured. Data are presented as means ± SEM. **P*<0.05 compared with A^y/+ control littermate group by one-way ANOVA.

Supplemental Figure 5. Aortic expressions of anti-oxidant enzymes were suppressed in E-DNIκB;A^y/+ mice

Aortic gene expressions of anti-oxidant enzymes from A^y/+ control (white bars, n=5) and E-DNIκB;A^y/+ (black bars, n=6) mice at 20 weeks of age were analyzed by RT-PCR. The relative amounts of mRNA were calculated with β-actin mRNA as the invariant control. Data are presented as means ± SEM. **P*<0.05, ***P*<0.01 compared with A^y/+ control littermate group by one-way ANOVA.

Supplemental Figure 6. Oxygen consumption during the dark phase was increased in E-DNIκB;A^y/+ mice

Oxygen consumption of A^y/+ control littermates (white bars, n=4) and E-DNIκB;A^y/+ mice (black bars, n=4) were measured at 16 weeks of age. Data are presented as means ± SEM. **P*<0.05 compared with A^y/+ control littermate group by one-way ANOVA.

Supplemental Figure 7. Protection from age-related body weight gain in E-DNIκB mice

(A) Food intakes of control (white bars, n=5) and E-DNIκB (black bars, n=6) of

50-week-old mice maintained on a normal chow diet. (B) Body weights of aged control and E-DNIκB mice at 50 weeks of age. Data are presented as means ± SEM. *P<0.05 compared with control littermate group by one-way ANOVA.

Supplemental Figure 8. eNOS deficiency suppresses the effects of endothelial DNIκB expression on blood pressure and muscle blood flow

(A) Blood pressures and (B) gastrocnemius muscle blood flows of wild-type, E-DNIκB, control $Nos3^{-/-}$ and E-DNIκB;$Nos3^{-/-}$ mice at 50-60 weeks of age. Data are presented as means ± SEM. *P<0.05 compared with control littermate group by one-way ANOVA. n=4-5 in each group.

Supplemental Figure 9. Schematic diagram illustrating the proposed functions of endothelial NF-κB signaling

Supplemental Table 1. Sequences of Quantitative RT-PCR primers

Supplemental Figure 1

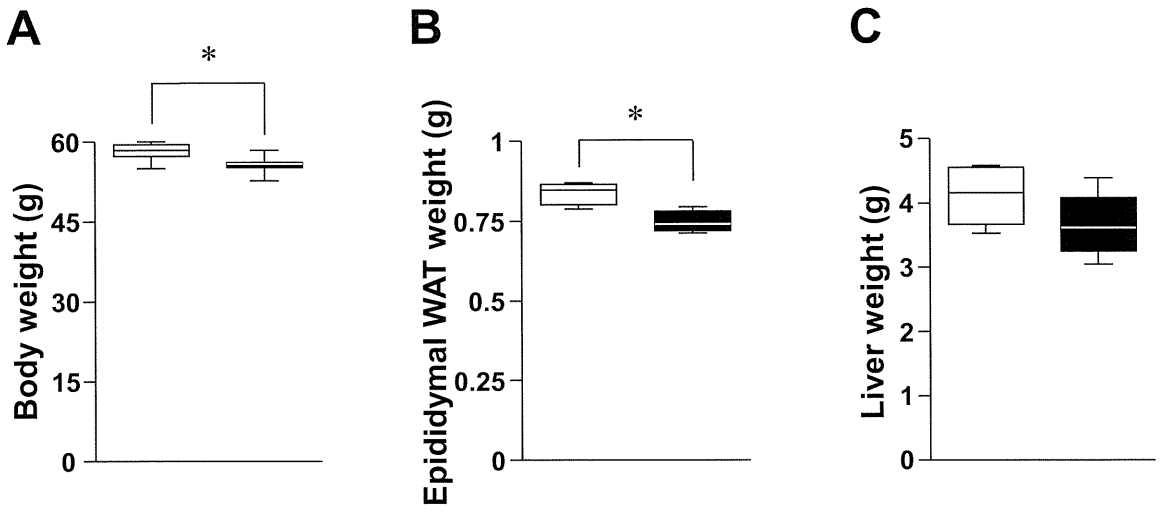

Supplemental Figure 2

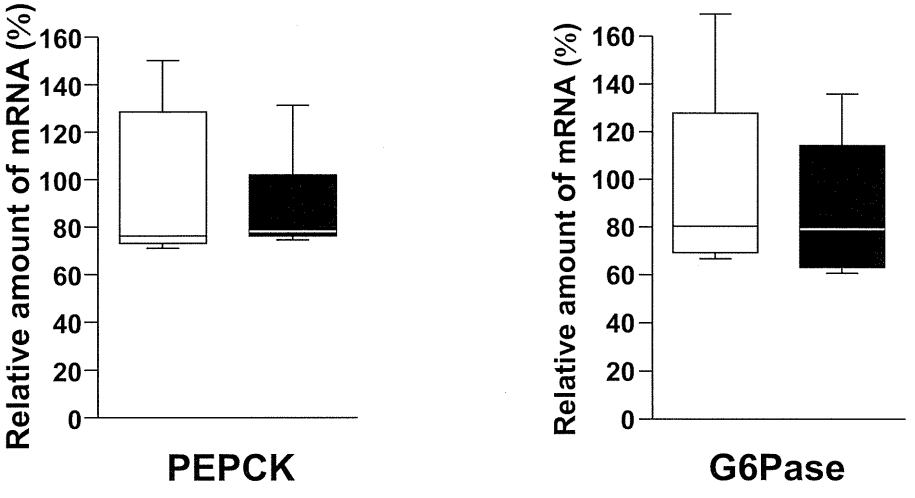

Supplemental Figure 3

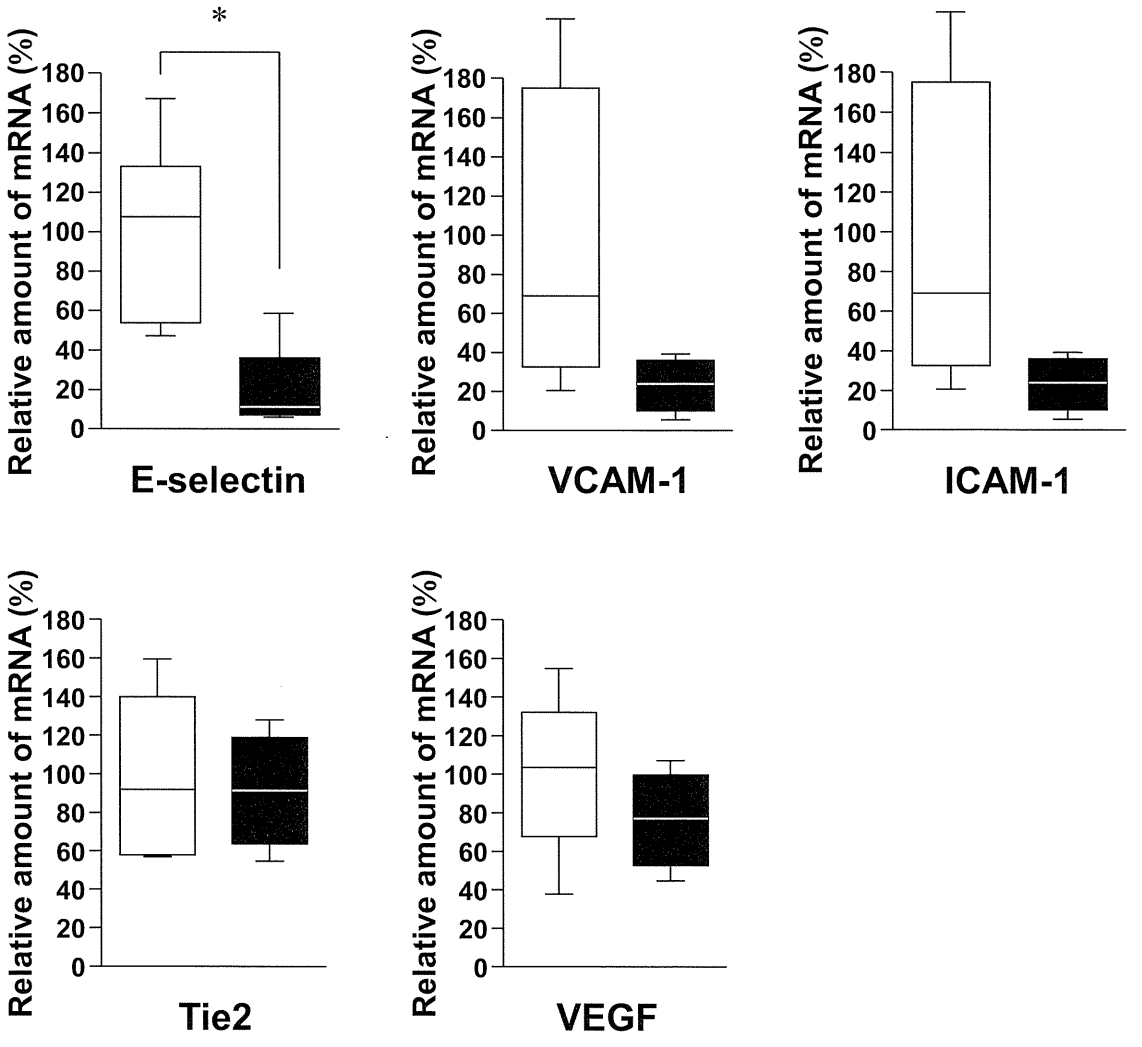

Supplemental Figure 4

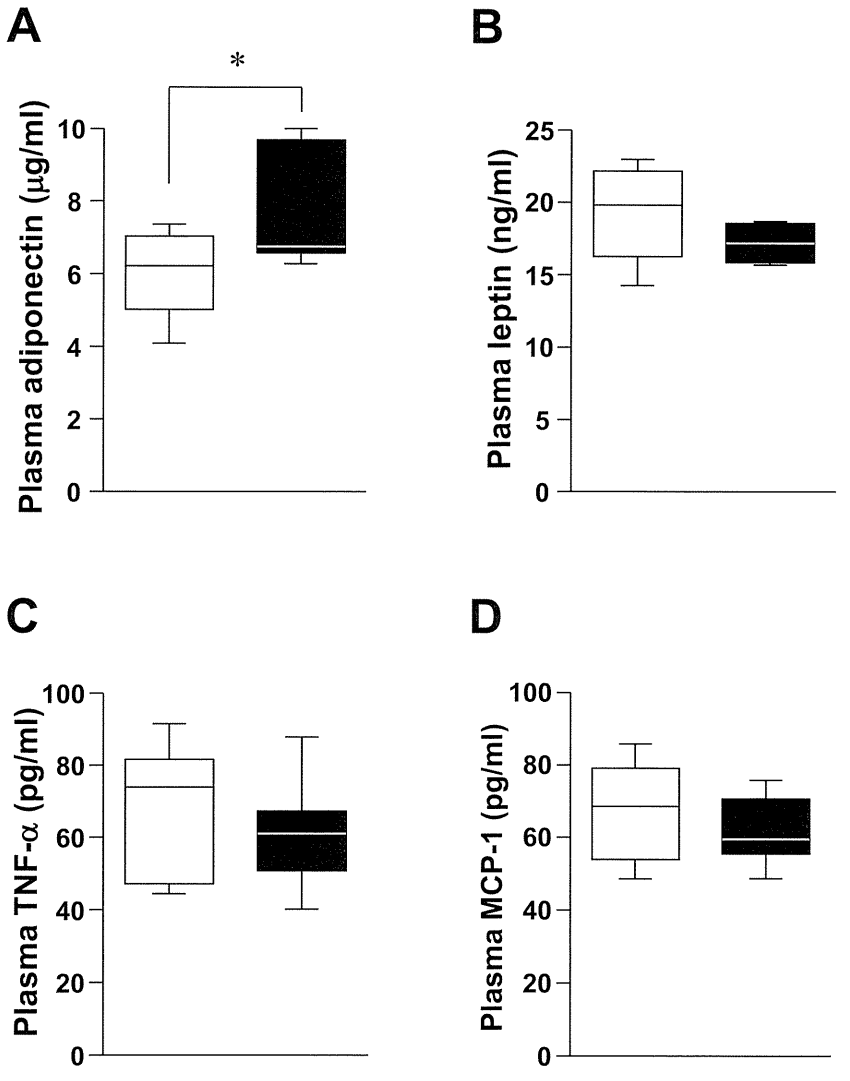

Supplemental Figure 5

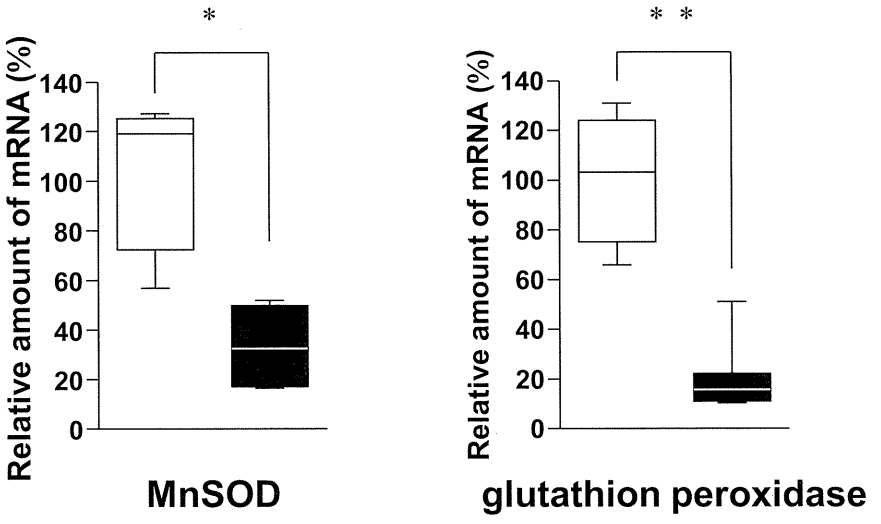

Supplemental Figure 6

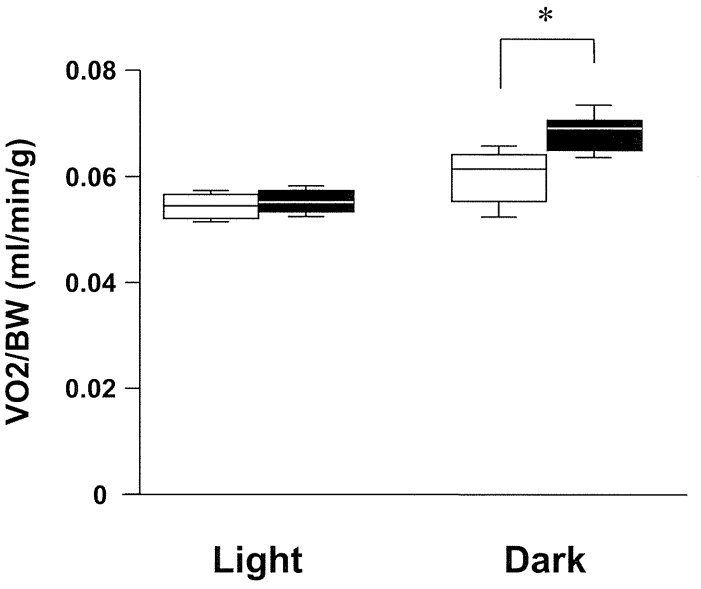

Supplemental Figure 7

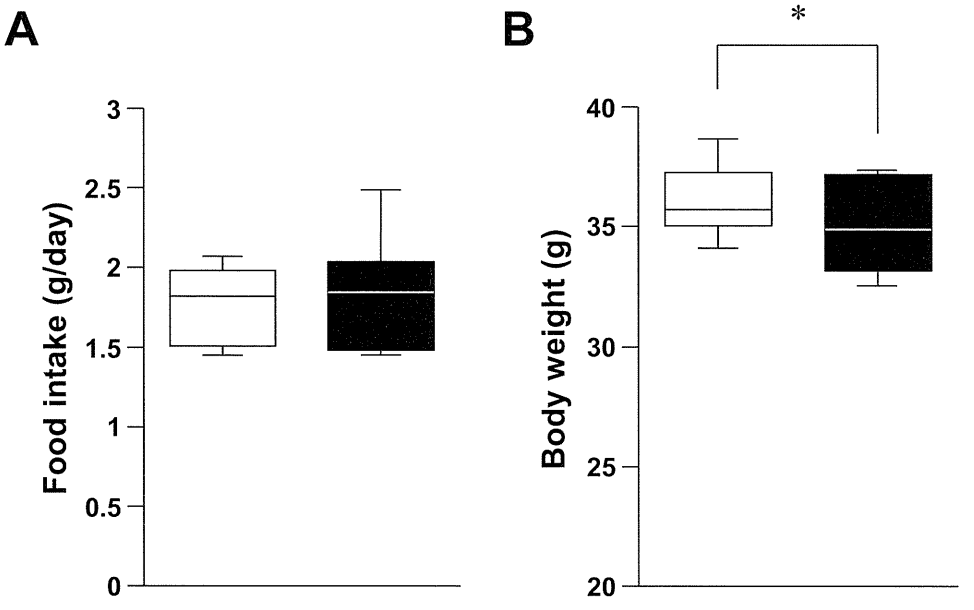

Supplemental Figure 8

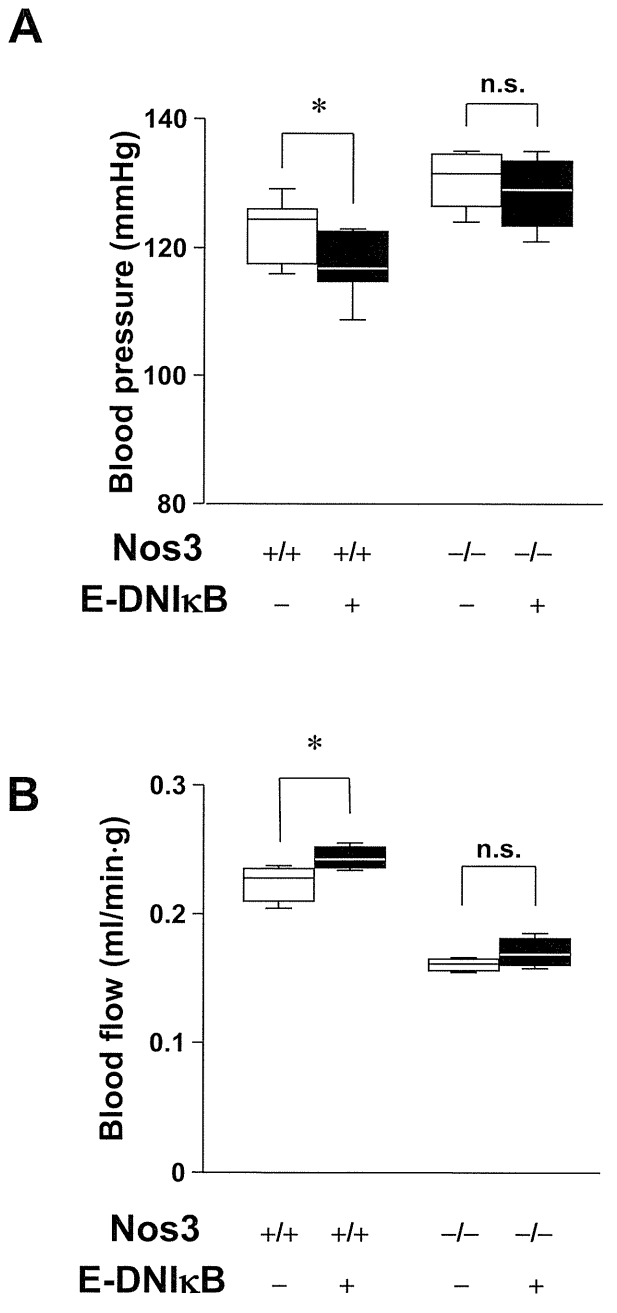

Supplemental Figure 9

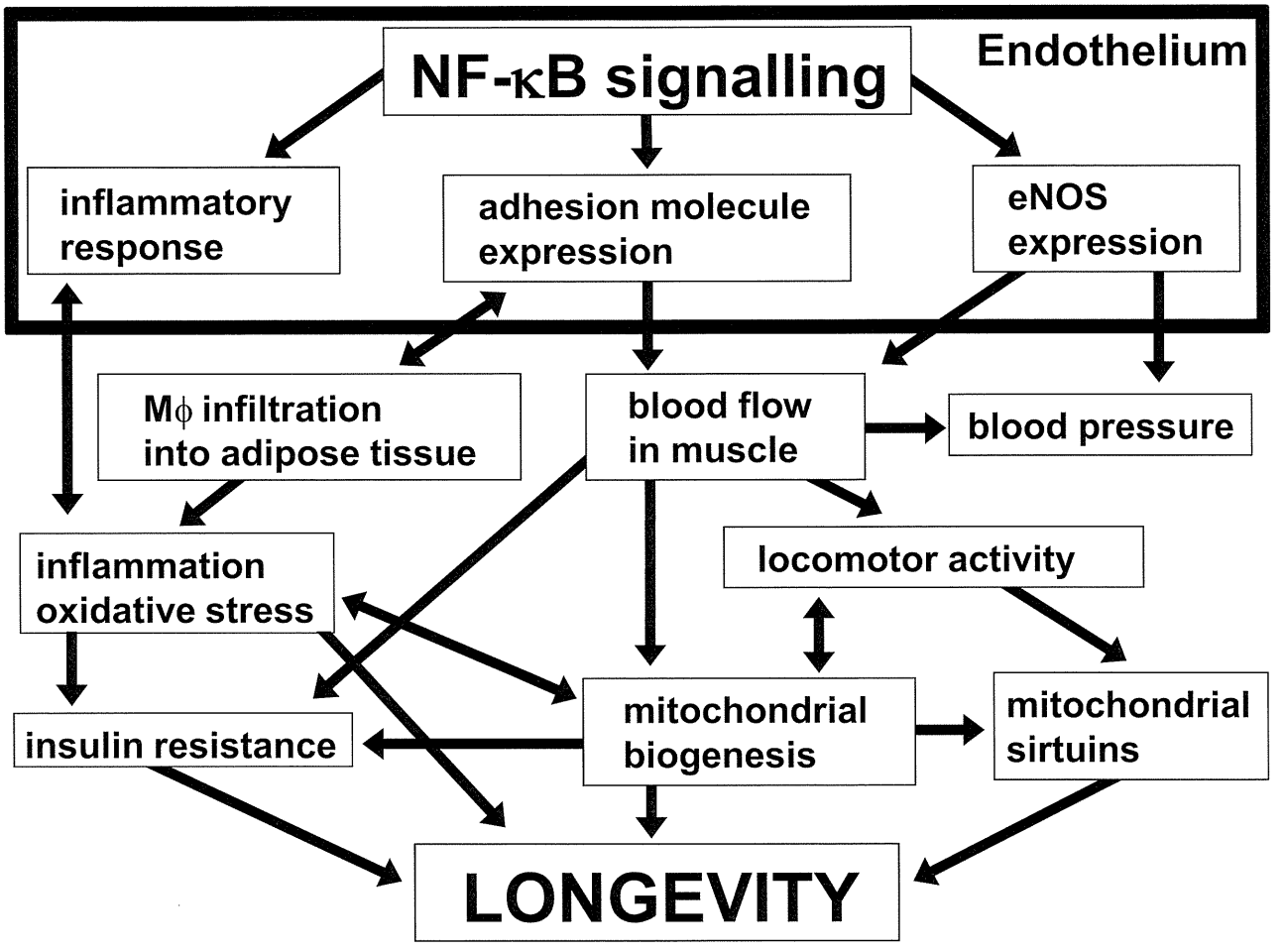

Supplemental Table 1

Probe	Primer 1	Primer 2
VCAM-1	GGA AGCTGGAACGAA GTA	CAATCTCCAGCCTGTAAACT
E-selectin	CATCGTCCTCATTGCTCTA	AGACGTTGTAAGAAGGCAC
eNOS	ATGTTTGTCTGCGGCGATGT	ATGTCCTCGTGGTAGCGTTG
F4/80	CATCATGGCATACCTGTTCAC	GAATGGGAGCTA AGGTCAGTC
iNOS	CAGCTGGGCTGTACAAACCTT	CATTGGAAGTGAAGCGTTTCG
Cytochrome C	GATTCTCTTACACAGATGCC	CTTCTTCTTAATTCCAGCGA
UCP-3	ATGCTGAAGATGGTGGCTC	CCGCAGTACCTGGACTTT
MCAD	TCGAAAGCGGCTCACAAGCAG	CACCGCAGCTTTCCGGAATGT
Nampt	AACGAAAGAGGATGGAACTAC	TACCAGGACTGAACAAGAATA
SIRT3	CTGCAAGGTTCCTACTCCA	CTTCGAGGACTCAGAACG
TNF-α	AGGTCAACGTTTCTGATTA	GGGTGGGTAGAATG
PEPCK	TTGCCTGGATGAAGTTTGAT	GGCATTTGGATTTGTCTTCACT
G6Pase	AAAGAGACTGTGGGCATCAATC	AATGCCTGACAAGACTCCAGCC
Tie2	CTTGTTGGCGTTTCTGATTA	TGATGTCATTCCAGTCAAGC
VEGF	TCATGCGGATCAAACCTCA	TTTCTGGCTTTGTTCTGTCTT
ICAM-1	GCTGCTACCTGCACTTTG	GGATGGATGGATACCTGA
Glutathion peroxidase	TGCAGAAGCGTCTGGGACCT	GGTCGGACGTACTTGAGGGA
MnSOD	GGTCGCTTACAGATTGCT	CTCCCAGTTGATTACATTCC
Alpha-actin	CAAATGCTTCTAAGTCCC	CCACGAGTAACAAATCAAAG
Beta-actin	TTGTAACCAACTGGGACGATATGG	GATCTTGATCTTCATGGTGCTAGG

METABOLISM CLINICAL AND EXPERIMENTAL XX (2012) XXX–XXX

Available at www.sciencedirect.com

Metabolism

www.metabolismjournal.com

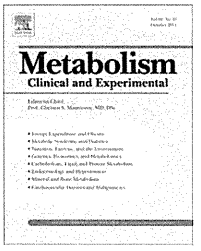

Atf6α-null mice are glucose intolerant due to pancreatic β-cell failure on a high-fat diet but partially resistant to diet-induced insulin resistance

Masahiro Usui[a], *Suguru Yamaguchi*[a,b], *Yasuhiro Tanji*[a], *Ryu Tominaga*[a], *Yasushi Ishigaki*[a], *Manabu Fukumoto*[c], *Hideki Katagiri*[d], *Kazutoshi Mori*[e], *Yoshitomo Oka*[a], *Hisamitsu Ishihara*[a,b,*]

[a] *Division of Molecular Metabolism and Diabetes, Tohoku University Graduate School of Medicine, Sendai 980-8575, Japan*
[b] *Division of Diabetes and Metabolism, Nihon University School of Medicine, Tokyo 173-8610, Japan*
[c] *Department of Pathology, Institute of Development, Aging and Cancer, Tohoku University Graduate School of Medicine, Sendai 980-8575, Japan*
[d] *Department of Metabolic Diseases, Center for Metabolic Diseases, Tohoku University Graduate School of Medicine, Sendai 980-8575, Japan*
[e] *Department of Biophysics, Graduate School of Science, Kyoto University, Kyoto 606-8502, Japan*

ARTICLE INFO

Article history:
Received 1 September 2011
Accepted 5 January 2012

ABSTRACT

Activating transcription factor 6α (ATF6α) is essential for the endoplasmic reticulum (ER) stress response. Since recent studies suggested that ER stress is involved in the pathogenesis of type 2 diabetes mellitus, we have analyzed *Atf6α*-null (*Atf6α*$^{-/-}$) mice challenged with metabolic overload or genetic manipulations. *Atf6α*$^{-/-}$ mice were fed a high-fat diet to create diet-induced obese (DO) mice, and were subjected to examination of glucose homeostasis with biochemical and morphological analysis of the pancreatic β-cell and liver tissues. *Atf6α*-null mice were also crossed with genetic models of diabetes caused either by insulin resistance (Agouti obese mice) or by impaired insulin secretion (*Ins2*$^{WT/C96Y}$ mice). *Atf6α*$^{-/-}$ DO mice were less glucose tolerant with blunted insulin secretion compared to littermates on a high-fat diet. Pancreatic insulin content was lower in *Atf6α*$^{-/-}$ DO mice with the swollen β-cell ER, a typical feature of cells with ER stress. In the liver of *Atf6α*$^{-/-}$ DO mice, XBP-1 splicing was increased, suggesting that higher ER stress was present. ATF6-deficient mice showed increased mRNA expressions of glucose-6-phosphatase and SREBP1c associated with a tendency for a higher degree of steatosis in the liver. However, *Atf6α*$^{-/-}$ DO mice exhibited higher insulin sensitivity with lower serum triglyceride levels. Similar phenotypes were observed in ATF6α-deficient Agouti mice. In addition, ATF6α-deficiency accelerated reduction in pancreatic insulin content in *Ins2*$^{WT/C96Y}$ mice. These data suggested that ATF6α contributes to both prevention and promotion of diabetes; it

Abbreviations: ATF6α, activating transcription factor 6α; BW, body weight; cDNA, complementary DNA; DO, diet-induced obese; eIF2α, eukaryotic initiation factor 2; ER, endoplasmic reticulum; G6Pase, glucose-6-phosphatase; GRP78, 78 kDa glucose-regulated protein; HFD, high-fat diet; IPGTT, intraperitoneal glucose tolerance test; ITT, intraperitoneal insulin tolerance test; IRE1, inositol requiring enzyme 1; PERK, PKR (double-stranded-RNA-dependent protein kinase)-like ER kinase; TG, triglyceride; UPR, unfolded protein response; VLDL, very low-density lipoprotein; WT, wild-type; XBP, X-box binding protein.

Authors' contributions: H.K., K.M., Y.O. and H.I. designed the research; M.U., S.Y., Y.T., R.T., and Y.I. performed the research; S.Y., Y.I., M.F., S.Y., and H.I. analyzed the data; M.U., Y.O., and H.I. wrote the paper.

* *Corresponding author.* Hisamitsu Ishihara, Division of Diabetes and Metabolism, Nihon University School of Medicine, Itabashi-ku, Tokyo 173-8610, Japan. Tel. +81 3 3972 8245; fax. +81 3 3972 8245.
E-mail address: ishihara.hisamitsu@nihon-u.ac.jp (H. Ishihara).

0026-0495/$ – see front matter
doi:10.1016/j.metabol.2012.01.004

Please cite this article as: Usui M, et al, Atf6α-null mice are glucose intolerant due to pancreatic β-cell failure on a high-fat diet but partially resistant to diet-induced..., Metabolism (2012), doi:10.1016/j.metabol.2012.01.004

protects β-cells from ER stress and suppresses hepatosteatosis, but plays a role in the development of hyperlipidemia and insulin resistance.

1. Introduction

Glucose homeostasis is maintained through fine regulation of insulin secretion from pancreatic β-cells and glucose production from the liver as well as glucose disposal into muscle and adipose tissues [1]. Recent studies have shown decreased pancreatic β-cell mass to be a common feature of subjects with type 2 diabetes mellitus (T2DM) [2-4]. Stress-mediated apoptosis is considered as one of the causes of β-cell loss. Pancreatic β-cells are especially vulnerable to endoplasmic reticulum (ER) stress [5,6] because of continuous and abundant production of insulin. In addition, ER stress and the activation of related stress signaling pathways are suggested to be an important mechanism underlying insulin resistance [7,8]. Recent studies showed that ER stress is present in adipose and liver tissues in obese humans [9-11].

ER stress is triggered when the amount of unfolded and misfolded proteins exceeds the folding capacity of the ER. This protein folding stress is recognized by three ER-resident transmembrane proteins, PERK (PKR (double-stranded-RNA-dependent protein kinase)-like ER kinase), IRE1 (inositol requiring enzyme 1) and ATF6α (activating transcription factor 6α). These ER stress sensor proteins initiate a series of signaling cascades known as the unfolded protein response (UPR) [12,13]. The UPR reduces ER stress in two ways, one of which is by reduction in ER protein load. This reduction is mediated by activation of PERK, which phosphorylates α subunit of eukaryotic translation initiation factor eIF2 (eIF2α), resulting in inhibition of global protein synthesis [14]. Another means to cope with ER stress is to increase protein folding capacity and to enhance activity of protein degradation. PERK-mediated inhibition of global protein synthesis paradoxically increases expression of ATF4. Activation of IRE1 leads to generation of an active form of transcription factor XBP-1 (X-box binding protein-1). These transcription factors together with ATF6α orchestrate transcriptional induction of specific genes which facilitate folding or degradation of misfolded proteins. Essential roles of PERK and IRE1α in cell survival have been established mainly through studies using *Perk*-null [15] and *Ire1α*-null [16] cells and mice. Furthermore, mutations of the *EIF2AK3* gene encoding PERK in humans cause Wolcott–Rallison syndrome with diabetes mellitus in early infancy [17], demonstrating an essential importance of PERK signaling in β-cells.

In contrast to these sub-pathways of the UPR, studies of the ATF6α-mediated pathway in the cell or organ physiology have recently been commenced. ATF6α is a type II transmembrane glycoprotein located on the ER membrane. In response to ER stress, ATF6α is cleaved and the N-terminus 50 kDa protein moves to the nucleus. Once in the nucleus ATF6α binds to the ER stress response elements in ER stress genes, which include molecular chaperones GRP78 and GRP94, augmenting ER capacity to assist folding of secretory and membrane proteins [13,18]. Recently, *Atf6α* knockout mice were generated [19,20]. Using cells from these mice, ATF6α was revealed to function as a critical regulator of ER quality control proteins.

In humans, expression of GRP78, a downstream effecter of ATF6α, was reportedly increased in T2DM β-cells [21]. Expressions of molecular chaperones downstream of ATF6α were also shown to be augmented in human adipose tissue and liver with obesity [10,11]. Furthermore, the ATF6α-Met67Val substitution with increased intrinsic activity was found to cause elevation in plasma cholesterol levels [22]. Several single nucleotide polymorphisms in the *ATF6α* gene were found to associate with T2DM [23-25], although a lack of association between genetic polymorphisms in the locus and glucose metabolism was also recently reported [26]. These data suggest an important role of ATF6α in development of obesity and T2DM. However, the causal relationship is not clear nor has the role of ATF6α been established in whole body glucose homeostasis. Therefore, in this study, we have analyzed glucose homeostasis in *Atf6α*-null mice challenged with metabolic overload or genetic manipulations.

2. Materials and methods

2.1. Animals

The Tohoku University Institutional Animal Care and Use Committee approved all animal experiments. Generation of *Atf6α*-null mice was described previously [20]. Heterozygous *Atf6α* knockout mice ($Atf6\alpha^{+/-}$) were backcrossed to female wild-type C57BL/6J mice eight times. Homozygous knockout mice were produced by intercrossing male and female heterozygotes. Genotyping for *Atf6α* knockout allele was performed using the forward primer 5′-CTTCTGAGGCGGAAAGAACCAGCTG-3′ and the reverse primer 5′-TTTGCAAGTC CAATGGGCC TCTC-3′. Reverse transcription PCR for detecting expression of *Atf6α* mRNA was conducted using primers 5′-CCAACAGAAAGCCGCATT-3′ and 5′-TGGACAGCCAT-CAGCTGA GA-3′. $Ins2^{WT/C96Y}$ (Akita) mice (C57BL/6J background, [27]) were purchased from Charles River. Male $Ins2^{WT/C96Y}$ mice were mated with female $Atf6\alpha^{-/-}$ mice to generate $Atf6\alpha^{+/-}Ins2^{WT/C96Y}$ mice which were further mated with female $Atf6\alpha^{-/-}$ to produce $Atf6\alpha^{-/-}Ins2^{WT/C96Y}$ mice. Genotyping for $Ins2^{WT/C96Y}$ mice was as described previously [27]. C57BL/6J Ham Slc-$A^{y/+}$(A^y) mice were obtained from Japan SLC. Male A^y mice were mated with female $Atf6\alpha^{-/-}$ mice to generate $Atf6\alpha^{+/-}A^y$ mice which were further mated with female $Atf6\alpha^{-/-}$ to produce $Atf6\alpha^{-/-}A^y$ mice. Offspring positive for the A^y gene were recognized by agouti coat color. All agouti experiments were performed on the F1 generation. The mice were kept under standard, specific pathogen-free conditions with a constant dark/light cycle and free access to standard

Please cite this article as: Usui M, et al, Atf6α-null mice are glucose intolerant due to pancreatic β-cell failure on a high-fat diet but partially resistant to diet-induced..., Metabolism (2012), doi:10.1016/j.metabol.2012.01.004

mouse chow (MF; Oriental Yeast, Tokyo, Japan) and water. The high-fat diet (rodent diet with 60% energy from fat; D12492) (HFD) was purchased from Research Diets (New Brunswick, NJ, USA) and was freely accessible.

2.2. Physiological studies

Body weights (BW) were measured once every other week. Blood samples were collected from the tail vein. Intraperitoneal glucose tolerance test (IPGTT: 2 g glucose/kg BW) was started by injecting 20% glucose solution. Intraperitoneal insulin tolerance test (ITT) was performed using the regular insulin (0.75 U/kg BW for mice on normal chow and 1.5 U/kg BW for mice on an HFD). Blood glucose levels were measured by the glucose oxidase method using a Glutest glucose sensor device (Sanwa Kagaku Kenkyusho, Nagoya, Japan). Serum insulin levels were determined using an insulin ELISA kit (Morinaga Institute of Biological Science, Tokyo, Japan).

2.3. Pancreatic insulin content and hepatic triglyceride content

Mice were killed by cervical dislocation. Pancreases were removed and homogenized in acid/ethanol (0.7 mol/l HCl/ethanol 25:75) and left at −20 °C for 48 h, with sonication every 24 h. Homogenates were then centrifuged (8000*g* for 10 min) and the insulin content of the acid/ethanol supernatant fraction was measured using insulin ELISA. Frozen livers were homogenized and triglycerides were extracted with CHCl3:CH3OH (2:1, v:v), dried and resuspended in 2-propanol [28]. Triglyceride content was measured using Lipidos liquid kit (TOYOBO, Osaka, Japan).

2.4. Immunohistochemistry

Pancreases were removed and fixed in 4% formalin. Formalin-fixed paraffin-embedded sections of pancreas were deparaffinized and re-hydrated. The sections were then incubated with a guinea pig anti-insulin IgG (DAKO Japan, Kyoto, Japan) diluted 1:1000 for 1 h at room temperature.

2.5. Quantitative RT-PCR

Total RNA was isolated from 0.05 g liver with Isogen (Wako Pure Chemical, Osaka, Japan), and cDNA was synthesized with a Transcriptor First Strand cDNA Synthesis Kit (Roche Diagnostics, Mannheim, Germany) using 1 μg total RNA. Complimentary DNA synthesized from total RNA was evaluated using the real-time quantitative PCR system (Light Cycler Quick System 350S; Roche Diagnostics). The relative amounts of mRNA were calculated with β-actin mRNA as the invariant control. The primers used are described in the Supplementary Table.

2.6. Ultrastructural analysis

We performed ultrastructural analyses of pancreatic β-cells from 25-week-old mice using electron microscopy. The samples of cells were fixed with 2% glutaraldehyde plus 2% paraformaldehyde in 0.1 M phosphate buffer (PB, pH 7.4) at 4 °C, and subsequently post-fixed with 2% osmium tetroxide in 0.1 M PB at 4 °C for 2 h. Then, the specimens were dehydrated in a graded ethanol, replaced in propylene oxide, and embedded in the epoxy resin. Ultrathin sections were obtained by ultramicrotomy technique. Ultrathin sections stained with uranyl acetate at 60 °C for 20 min and modified Sato's lead solution for 5 min were submitted to transmission electron microscope observation (JEM-1200EX, JEOL). The β-cells were distinguished from α- and δ-cells by the appearance of their secretory granules. The β-cell granules had a white halo, not evident in α- and δ-cell granules.

2.7. Statistical analysis

Data are presented as means ± S.E., unless otherwise indicated. Differences between groups were assessed by Student's *t* test.

3. Results

3.1. Glucose homeostasis in ATF6α-deficient mice on normal chow

Founder *Atf6α* heterozygous knockout mice [20] were backcrossed to the C57BL/6J mice for at least 8 generations and heterozygous knockout male and female mice were mated to generate whole body *Atf6α* homo knockout mice (Fig. 1A). In the present study, we analyzed male mice, since preliminary studies showed similar phenotypes in female *Atf6α*$^{-/-}$ mice. When *Atf6α*-null mice were fed with standard chow, their body weights (BW) tended to be lower than those of wild-type (WT) mice (Fig. 1B). Blood glucose levels measured in non-fasted states were comparable between two strains (data not shown). Neither blood glucose excursions (Fig. 1C) nor insulin secretory responses (Fig. 1D) differed significantly between WT and *Atf6α*$^{-/-}$ mice when mice were subjected to an intraperitoneal glucose tolerance test (IPGTT). Insulin sensitivity, estimated by an intraperitoneal insulin (0.75 U/kg BW) tolerance test (ITT), showed that *Atf6α*$^{-/-}$ mice were somewhat more insulin sensitive, although the difference was not statistically significant (Fig. 1E). However, when ITT was performed using 2.0 U/kg BW of insulin, 5 out of 6 *Atf6α*$^{-/-}$ mice showed severe hypoglycemia of less than the lower detection limit (1.1 mM) of the glucose monitoring device at 60, and 90 min, while blood glucose levels of all WT mice were higher than 2.0 mM at 90 min (Fig. 1F), suggesting that insulin sensitivity were higher in *Atf6α*$^{-/-}$ than in WT littermates.

3.2. Glucose homeostasis in ATF6α-deficient mice fed with a high fat diet

Impaired glucose homeostasis is often associated with obesity. To further investigate roles of ATF6α in glucose homeostasis, we fed *Atf6α*$^{-/-}$ mice with a 60% high fat diet (HFD) to generate diet-induced obese (DO) animals. ATF6α-

Please cite this article as: Usui M, et al, Atf6α-null mice are glucose intolerant due to pancreatic β-cell failure on a high-fat diet but partially resistant to diet-induced..., Metabolism (2012), doi:10.1016/j.metabol.2012.01.004